Pure Appl. Chem., Vol. 77, No. 8, pp. 1297–1315, 2005.
DOI: 10.1351/pac200577081297

Advanced experimental techniques in polymer thermodynamics*

Jean-Pierre E. Grolier

Laboratoire de Thermodynamique des Solutions et des Polymères, Université Blaise Pascal, 63177 Aubière, France

Abstract: Scanning transitiometry is at the center of several new developments to generate original unprecedented data over extended ranges of temperatures and pressures. Simultaneous in situ spectroscopic readings noticeably extend the performance of scanning transitiometry. The modulation of temperature superimposed to temperature scanning for thermal analysis is a major step forward to unambiguously identify glass transitions from other overlapping phenomena. The combination of a weighing technique (vibrating-wire technique) with a pressure decay technique (*pVT* technique) allows us to estimate simultaneously, in situ on the same polymer sample, the gas solubility and the concomitant polymer swelling.

Keywords: Scanning transitiometry; temperature-modulated DSC; vibrating-wire technique; glass transition; particle synthesis; high pressure.

INTRODUCTION

Research in polymer science continues to develop actively, producing numerous new elastomers, plastics, adhesives, coatings, and fibers. Thus, the ideas of thermodynamics, kinetics, and polymer chain structure work together to strengthen the field of polymer science. In many industrial applications, during extrusion processing or as all-purpose materials, polymers are usually submitted to extreme conditions of temperature and pressure. Furthermore, they are also very often in contact with gases and fluids, either as on-duty materials (containers, pipes) or as process intermediates (foaming, molding). The broad field of polymeric materials currently witnesses an impressive acceleration of activities. New advanced materials are constantly appearing. The materials that will be used or needed in the next decade are not even known yet. Since such materials are often used in special environments or under extreme conditions of temperature and pressure, their careful characterization must be done not only at the early stage of their development, but also all along their life cycle. Furthermore, their properties as functions of temperature and pressure must be well established for the optimal control of their processability. This also stands for phase transitions; ignorance of a phase diagram, particularly at extreme conditions of pressure, temperature, and chemical reactivity, is a limiting factor to the development of an industrial process (e.g., sol-gel transitions, polymerization under solvent near-supercritical conditions, and micro- and nanofoaming processes). Undoubtedly, thermal and calorimetric techniques are essential in this respect. In relating thermal as well as mechanical behavior to materials' structures, these techniques are perfectly adapted to provide accurate data in wide ranges of temperature and pressure.

*Paper based on the Rossini lecture at the 18th IUPAC International Conference on Chemical Thermodynamics (ICCT-2004), 17–21 August 2004, Beijing, China. Other presentations are published in this issue, pp. 1297–1444.

Typically, thermophysical properties feature the most important information expected when dealing with materials submitted to thermal variations and/or mechanical constraints. The properties of interest are of two types, bulk properties and phase-transition properties. The bulk properties are either caloric properties, such as heat capacities C_P, and mechanical properties, such as isobaric thermal expansivities α_P, isothermal compressibilities κ_T, and isochoric thermal pressure coefficients β_V. The two main thermal properties concern the first-order transitions, fusion and crystallization, and the glass transition. All these properties are now accessible thanks to recent progress in experimental techniques that allow measurements in the three physical states over extended ranges of T and p, including in the vicinity of the critical point (at least in the case of gases and liquids). In this respect, knowledge (i.e., measurements) of the thermophysical properties of polymers over extended ranges of temperature and pressures and in different gaseous environments is undoubtedly necessary to improve the use and lifetime of end-products made of such polymers. Knowledge of gas solubility and gas diffusivity in polymers as well as swelling capability is essential in many areas and requires information evidently on the type and extent of the interactions between the polymer and the gas.

The first section of this paper reviews newly developed techniques that have recently given noticeable impetus to investigations in polymer thermophysics and polymer physical chemistry; the basic principles and the latest improvements in experimental techniques will be described. The second section includes selected examples that illustrate how such techniques have worked together to provide valuable data for significant progress in polymer science.

EXPERIMENTAL TECHNIQUES

Calorimetry is certainly a major technique to measure thermodynamic properties of substances and to follow phase change phenomena or chemical reactions. In most applications, calorimetry is carried out at constant pressure while the tracked phenomenon is observed on increasing or decreasing the temperature or the adding of a reactant (either stepwise or at a constant scanning rate). The possibility of controlling the three most important thermodynamic variables (p, V, and T) in calorimetric measurements makes it possible to perform simultaneous measurements of both thermal and mechanical contributions to the thermodynamic potential changes caused by the perturbation. Calorimetric techniques provide valuable additional information on transitions in complex systems. Their contributions to the total change of thermodynamic potential not only leads to the complete thermodynamic description of the system under study, but also permits investigation of systems with limited stability or systems with irreversible transitions. By a proper external change of the controlling variable, the course of a transition under investigation can be accelerated, impeded, or even stopped at any degree of its advancement and then taken back to the beginning, all with simultaneous recording of the heat and mechanical variable variations.

Newly developed technologies in *pVT*-scanning calorimetry and in spectrocalorimetry have yielded a series of instruments that help to investigate in depth temperature and pressure effects on fundamental physical chemistry phenomena as well as on industrial processes. When dealing with polymer materials, the glass transition must be unambiguously established, in particular with respect to its dependence with temperature, pressure, and plasticizers, especially gases. Modulated techniques such as temperature-modulated thermal analysis are essential in this respect. As regards gas–polymer interactions, both the amount of gas absorbed/solubilized and the concomitant polymer swelling have to be precisely evaluated. In the following subsection, scanning transitiometry, temperature-modulated differential scanning calorimetry (TMDSC), and gas solubility are reviewed.

Scanning transitiometry

The seminal presentation by Randzio [1] of thermodynamic fundamentals for the use of state variables (p,V,T) in scanning calorimetric measurements has opened the path [2–4] from p,V,T calorimetry to the

now well-established scanning transitiometry technique [5]. With this technique, the simultaneous determination of thermal and mechanical responses of the investigated system, perturbated by a variation of an independent thermodynamic variable while the other independent variable is kept automatically constant, results in the determination of thermodynamic derivatives over extended ranges of pressure and temperature, impossible to obtain by other known techniques. Four thermodynamic situations are thus possible to realize in the instruments based on such techniques, namely, *pVT*-controlled scanning calorimeters or simply scanning transitiometers, since they are particularly adapted to investigate transitions by scanning one of the three thermodynamic variables. The four possible thermodynamic situations are obtained by simultaneous recording of both heat flow (thermal output) and the change of the dependable variable (mechanical output). Then, making use of the respective related Maxwell relations one readily obtains the main thermophysical properties as follows: (a) scanning pressure under isothermal conditions yields the isobaric thermal expansivity α_P and the isothermal compressibility κ_T as functions of pressure at a given temperature; (b) scanning volume under isothermal conditions yields the isochoric thermal pressure coefficient β_V and the isothermal compressibility κ_T as functions of volume at a given temperature; (c) scanning temperature under isobaric conditions yields the isobaric heat capacity C_P and the isobaric thermal expansivity α_P; (d) scanning temperature under isochoric conditions yields the isochoric heat capacity C_V and the isochoric thermal pressure coefficient β_V.

A detailed description of a basic scanning transitiometer is given elsewhere [6]. A detailed scheme of the instruments (from BGR TECH, Warsaw, Poland) used in the present applications to polymers and constructed according to the principle of scanning transitiometry is presented in Fig. 1. It consists of a calorimeter equipped with high-pressure vessels, a *pVT* system, and a LabVIEW-based virtual instrument (VI) software. Two cylindrical calorimetric detectors (ext. diameter 17 mm, length 80 mm) made from 622 thermocouples chromel-alumel each are mounted differentially and connected to a nanovolt amplifier. The calorimetric detectors are placed in a calorimetric metallic block, the temperature of which is directly controlled with an entirely digital feedback loop of 22-bit resolution (~10^{-4} K), being part of the transitiometer software. The calorimetric block is surrounded by a heating–cooling shield connected to an ultracryostat (Unistat 385 from Huber, Germany) and the temperature difference between the block and the heating–cooling shield is set constant (5, 10, 20, or 30 K) as controlled by an analogue additional controller. The whole assembly is placed in a thermal insulation enclosed in a stainless steel body and placed on a stand, which permits to move the calorimeter up and down over the calorimetric vessels. The actual operating ranges of scanning transitiometry are respectively 173 K < T < 673 K and 0.1 MPa < p < 200 MPa (or 400 MPa).

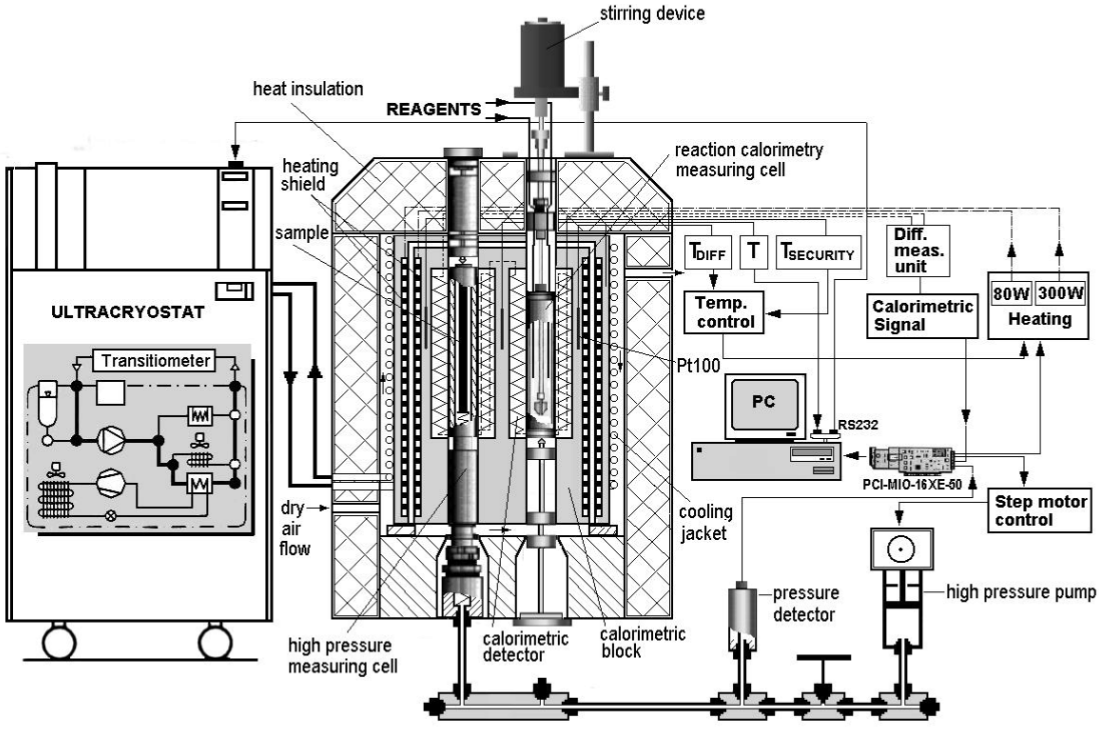

Fig. 1 Detailed scheme of a transitiometer set-up for simultaneous in situ analysis of thermal and volumetric properties of polymers at pressures up to 200 MPa, over the temperature range from 173 to 570 K. For convenience, two types of cells are shown (on the left-hand side is the high-pressure cell and on the right-hand side is the reaction cell).

As a matter of fact, transitiometry is at the center of several experimental techniques since with such equipments, bulk properties, transitions as well as reactions (e.g., polymerization) can be advantageously studied. In the case of a nonreacting system that remains in a homogeneous state, both the mechanical and thermal outputs as explained before give straightforward access to pairs of the thermomechanical coefficients. When the system or the material sample goes through a chemical reaction or a phase change, the recorded information yields the corresponding heat and *pVT* characteristics. In the case of polymer synthesis, a scanning transitiometer is used as an isothermal reaction calorimeter, the advancement of a polymerization reaction being accurately monitored through the rigorous control of the thermodynamic parameters [7]. Two reaction cells—measuring and reference—are made as equal as possible to each other, and they operate in a common surroundings in a so-called *twin differential* arrangement. The thermocouples composing the fluxmeters serve as a heat conduction path between cell walls and the block. The overall thermoelectric voltage, E, generated at the junctions provides an error-free indication of the temperature difference, which causes the heat flux along the wires; the overall heat flux (thermal power), W, is summed up by series arrangement of the individual thermocouples. The thermoelectromotive force is related to the thermal power by the following relation:

$$E = k \cdot W \tag{1}$$

where k is a calibration constant which depends on the thermoelectric capacity, ε, and conductance, γ, of the thermocouple wires. To gather additional information on a reaction, reaction calorimeters are often coupled with other analytical devices (e.g., online Fourier transform infrared, particle sizing probes, turbidity probes, pH or other ion selective probes, etc.). Therefore, we developed a reaction cell

which allows stirring, different dosing profiles for one or two reactants, and can accommodate a small optical probe coupled to a miniaturized spectrometer, Fig. 2.

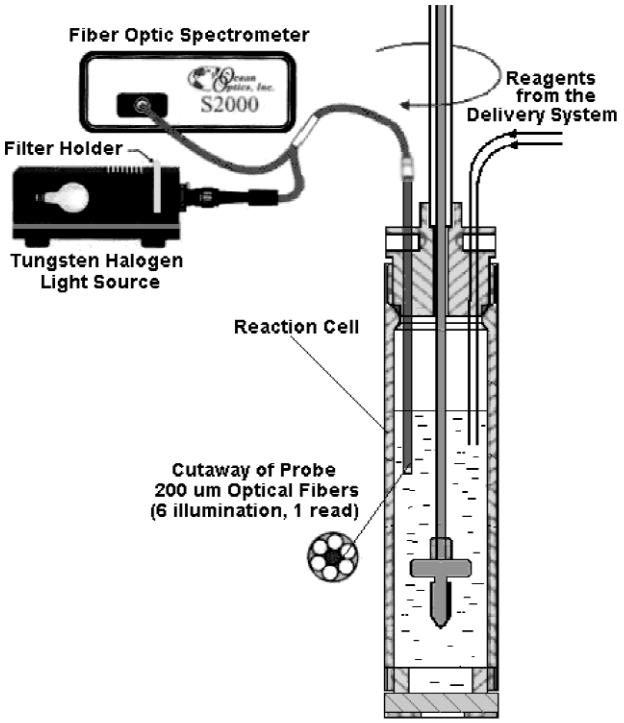

Fig. 2 Reaction-type cell used in the transitiometer. It shows different parts, the special stirrer, capillaries for reagents delivery, fiber optic probe connecting to spectrometer.

The performances of these versatile instruments will be illustrated in subsequent sections.

Temperature-modulated differential scanning calorimetry

The rapid evolution of both methodology and technology has led to recent applications of temperature-modulated calorimetry, particularly the combination of the technique with differential scanning calorimetry [8]. Different terms such as "periodic", "oscillating", "dynamic", or "alternating" have thus been used to described similar techniques based on different types of instruments. The use of TMDSC to characterize polymers deals mostly with detection of weak transitions, determination of heat capacities in quasi-isothermal mode, and separation of superimposed phenomena. The mathematical development necessary to describe the technique is well known [8], and different approaches have been proposed [9]. The total differential heat flow obtained after deconvolution of the modulated heat flow represents the sum of two distinguishable contributions, because the response to the imposed temperature modulation is different depending on the phenomena submitted to the temperature changes. One component, called reversing heat flow, is linked to the heat capacity change; the modifications that depend on the temperature scanning rate can be cycled by alternating heating and cooling effects. The second component is linked to the kinetics and is called non-reversing heat flow, by opposition to the first one; modifications appearing in this signal depend only on the temperature.

The specific heat capacity c_p measured with a conventional DSC, under the conditions of negligible temperature gradient within the sample, is approximately proportional to the temperature difference between the sample and the reference or to the heat flow difference. Calculation of the sample heat

capacity is possible through calibration data, at the working temperature, via the following relation (m and m Al_2O_3 are respectively the mass of the sample and the mass of sapphire used as standard calibrating substance):

$$m\,c_p = m_{Al_2O_3}\,c_{p(Al_2O_3)}\,\frac{a_s - a_b}{a_c - a_b} \tag{2}$$

where the quantities a represent the amplitudes of the heat flow (or temperature) differences signals for different situations corresponding to: sample, calibration and baseline runs designated respectively by "s", "c", and "b". Usually, the baseline run (a_b) is obtained with two empty aluminum pans. In a measuring run (a_s), the sample is in one of the aluminum pans, whereas in the calibration run (a_c), the sample is replaced by the standard sapphire (Al_2O_3), having a well-known specific heat capacity. In the case of TMDSC, the calibration equation takes the form

$$\left(C_s - C_r\right) = \frac{A_\Delta}{A_{Ts}}\sqrt{\left(\frac{K}{\omega}\right)^2 + C_r^2} \tag{3}$$

where C_s and C_r represent the heat capacities of the sample and of the reference, respectively (these quantities include the contribution of the sample and of the pans which can be regarded as identical on the two sides), A_Δ is the temperature difference amplitude between sample and reference, A_{Ts} is the sample temperature amplitude (in Kelvin), and ω designates the modulation frequency (=$2\pi/p$ with p being the modulation period in s). K is the temperature-dependent Newton's law constant. When calibrating with sapphire, eq. 3 leads to the following equation:

$$\left(C_s - C_r\right) = K_{Cp}\,\frac{A_{HF}}{\omega\,A_{Ts}} \tag{4}$$

where A_{HF} refers to the amplitude of the differential heat flow, and K_{Cp} is the calibration constant for heat capacity measurements. The heat capacity of the sample obtained using eq. 4 allows the determination of the contributions of the reversing and of the non-reversing heat flows, respectively, noted HF_{rev} and $HF_{non\text{-}rev}$, to the total heat flow HF_{tot} using the following relations:

HF_{rev} signal = average temperature scanning rate × heat capacity signal (conventionally, on heating a negative sign is necessary because an endothermic effect in the sample, i.e., heat consumption, creates a negative ΔT between the sample and the reference) then, $HF_{non\text{-}rev}$ signal = HF_{tot} signal – HF_{rev} signal.

One of the major advantages of the technique described above is most probably the possibility to access directly in a single run to overlapping effects. In this respect, TMDSC appears to be a more powerful technique than standard DSC. The thermal analyzer used in the present work is a Mettler DSC 821 equipped with a refrigerating cooling system RP 100 (from LabPlant, UK) allowing us to work from 200 to 700 K.

One example will serve to illustrate the high potentiality of the technique to detect unambiguously polymer glass transitions.

Vibrating-wire (VW)-*pVT* technique for gas solubility and polymer swelling

The understanding of {gas–polymer} interactions is essential in many industrial applications of thermoplastic polymers. This is the case where such polymers are processed (foaming, extrusion, molding) to produce end-products. This is also particularly the case in the petroleum industry where these polymers are used as materials for making pipelines or seals. In all cases, polymers are usually submitted to gas sorption under elevated temperatures and high pressures. In this respect, a quantitative evaluation of the amount of gases (often in supercritical state) in the polymers is of paramount importance.

In order to investigate possible hysteresis phenomenon between sorption and desorption, both sorption (measurements made as the experimental pressure is increased) and desorption (measurements made as the experimental pressure is decreased) are preferably performed. For this purpose, isotherms are obtained using a concept that has the particularity to combine two techniques [10], a VW sensor and a pressure decay *pVT* technique. The VW sensor is employed as a force sensor to weigh the polymer sample during the sorption: the buoyancy force exerted by the pressurized fluid on the polymer depends on the swollen volume, ΔV_{pol}, of the polymer due to the gas sorption. This VW sensor is essentially a high-pressure cell in which the polymer sample is placed in a holder suspended by a thin tungsten wire (diameter 25 μm, length 30 m) in such a way that the wire is positioned in the middle of a high magnetic field generated by a square magnet placed across the high-pressure cell. Through appropriate electric circuitry and electronic control, the tungsten wire is activated to vibrate. The period of vibration which can be accurately measured is directly related to the mass of the suspended sample. The pressure decay *pVT* method allows us to calculate the number of moles, n_{sol}, of gas (which is initially kept in a high-pressure calibrated cell) absorbed in the polymer, from the measurement of pressure at its initial value p_i when the gas enters the measuring cell and its final value p_f after the gas–polymer system has returned to thermodynamic equilibrium. The combined VW-*pVT* apparatus is designed to measure sorption of gases and the concomitant volume change of polymers at pressures up to 100 MPa from room temperature to 473 K. The experimental method consists of a series of successive transfers of the gas by connecting the calibrated cell to the equilibrium cell that contains the polymer. The initial, p_i, and final, p_f, pressures are recorded between each transfer. The initial methodology was based on the iterative calculation described by Hilic et al. [10,11]. The iterative operation was designed to simultaneously calculate the solubility and the volume change of the polymer due to sorption, using two rigorous working equations. However, a careful check of the whole procedure showed that the two working equations do not converge.

The working eq. 5 for the *pVT* technique gives the amount of gas entering the polymer sample during the first transfer once equilibration is attained

$$m_{\mathrm{sol}} = \frac{M_g}{RT_f}\frac{p_f}{Z_f}\Delta V_{\mathrm{pol}} + \frac{M_g}{R}\left[\frac{p_i}{Z_i T_i}V_3 - \frac{p_f}{Z_f T_f}\left(V_2 + V_3 - V_{\mathrm{pol}}\right)\right] \tag{5}$$

The term m_{sol} is the mass of gas dissolved in the polymer, M_g is the molar mass of the dissolved gas, Z_i with Z_f are the compression factors of the gas entering the polymer respectively at the initial (index $_i$) and final (equilibrium sorption, index $_f$) conditions. Volume of the degassed polymer and the volume change due to sorption are represented by V_{pol} and ΔV_{pol}, respectively. And the total amount of gas absorbed by the polymer after completion of the successive transfers is given by eq. 6

$$\Delta m_{\mathrm{sol}}^{(k)} = \frac{M_g}{R}\frac{p_f^{(k)}\Delta V_{\mathrm{pol}}^{(k)}}{Z_f^{(k)}T_f^{(k)}} + \frac{M_g}{R}\left[\frac{p_i^{(k)}V_3}{Z_i^{(k)}T_i^{(k)}} + \frac{p_f^{(k-1)}\left(V_2 - V_p - \Delta V_{\mathrm{pol}}^{(k-1)}\right)}{Z_f^{(k-1)}T_f^{(k-1)}} - \frac{p_f^{(k)}\left(V_2 + V_3 - V_{\mathrm{pol}}\right)}{Z_f^{(k)}T_f^{(k)}}\right] \tag{6}$$

where $\Delta m_{\mathrm{sol}}^{(\mathrm{k})}$ is the increment in dissolved gas mass resulting from the transfer k and $\Delta V_{\mathrm{pol}}^{(\mathrm{k})}$ is the change in volume after transfer k.

The working eq. 7 for the VW sensor relates the mass, m_{sol}, of gas absorbed in the polymer to the change in volume, ΔV_{pol}, of the polymer. The natural angular frequency of the wire, through which the

polymer sample holder is suspended, depends on the amount of gas absorbed. The physical characteristics of the wire are accounted for in eq. 7 as:

$$m_{\mathrm{sol}} = \rho \Delta V_{\mathrm{pol}} + \left[\left(\omega_{\mathrm{B}}^2 - \omega_0^2 \right) \frac{4L^2 R^2 \rho s}{\pi g} + \rho \left(V_{\mathrm{C}} + V_{\mathrm{pol}} \right) \right] \tag{7}$$

The terms ω_0 with ω_{B} represent the natural (angular) frequencies of the wire in vacuum and under pressure respectively, V_{C} the volume of the container. The symbols L, R, and ρs are respectively the length, the radius, and the density of the wire.

A common term appears in both eqs. 6 and 7, the density, ρ, of the gas

$$\rho_{\mathrm{gas}} = \frac{M_g}{RT} \frac{p_f}{Z_f} \tag{8}$$

Then, eq. 7 can be written

$$\Delta m_{\mathrm{sol}}^{(k)} = \rho_{\mathrm{gas}} \, \Delta V_{\mathrm{pol}} + d \tag{9}$$

The term d represents the apparent concentration of gas in the polymer, i.e. when the change in volume, ΔV_{pol}, is zero. However, despite the different terms appearing in the two working eqs. 6 and 7, these two equations can be both expressed by the same reduced eq. 9 having the slope given by eq. 8. The VW sensor is described with rigorous models yielding a working equation in which all parameters have a physical meaning: ω_0 and ω_{B} the natural frequencies [Hz], V_{C} [m^3], L [m], R [m], and ρs [kg m^{-3}] of the wire. The pressure decay technique requires Z, M_g [g mol^{-1}] for the gas and the volumes of the cells [m^3]. The volume of the polymer sample, V_{pol}, with its associated change, ΔV_{pol}, and the total mass of dissolved gas, m_{sol}, are the only unknown terms.

It appears that the VW sensor technique is more precise than the *pVT* technique because there are no cumulative errors as in the case of the *pVT* method, when the successive transfers are performed during an isothermal sorption. The technique does not require extensive calibrations. Essentially, uncertainties come from the experimentally measured resonance frequencies. Errors are reduced with the new data acquisition permitting the simultaneous recording of the phase with the frequency: effectively, the phase angle is better suited than the amplitude to detect the natural resonant frequency (and also the half-width) [12]. The main source of uncertainty affecting the evaluation of the gas concentration data comes from the term of eq. 9, which contains the density of the gas and the change in volume of the polymer. At this stage, it was then necessary to elaborate a new procedure to unambiguously obtain the apparent solubility of the gas in the polymer and the associated change in volume. For this, the Sanchez–Lacombe equation of state (SL-EOS) was selected to estimate the change in volume of the polymer at different pressures and temperatures [12].

SELECTED RESULTS

Performances and advantages of scanning transitiometry in polymer science are well demonstrated by typical applications in several important fields: (i) transitions of polymer systems under various constraints (temperature, pressure, gas sorption) including first-order phase transitions [13,14] and biopolymer gelatinization [15–17]; (ii) polymer thermophysical properties and influence of gas sorption [14,18]; (iii) anionic polymerization [14,19,20]. In what follows, two examples have been selected, namely: *glass-transition temperature of elastomers under high pressure* and *polymer particle synthesis using spectrotransitiometry*.

The great selectivity of TMDSC for asserting glass-transition temperatures T_g has been shown in the case of resins used for nanolithography, in several microelectronics applications [see, e.g., refs.

21–23] and in the case of polymers used for polymer foaming [24]. This TMDSC selectivity will be illustrated with one example: *T_g determination by TMDSC of polystyrene (PS) modified by high-pressure methane*.

The simultaneous determination of gas solubility in a polymer and the concomitant swelling of the polymer is certainly a new advance in the investigation of gas–polymer interactions. Experimental and technological improvements as well as associated methodology are still under active developments, however, significant results have been obtained for solubilities of nitrogen N_2, carbon dioxide CO_2, and two hydrofluorocarbons, HFC134-a and HFC152-a, in PS [11,25]. The coupled VW-*pVT* technique has been recently revisited [12], and this activity will be illustrated with one example: *CO_2 solubilities in medium-density polyethylene (MDPE) and poly(vinylidene fluoride) (PVDF).*

Glass-transition temperatures of elastomers under high pressure

The glass-transition temperature is affected by pressure since an increase of pressure causes a decrease in the total volume, and an increase in T_g is expected due to the decrease of free volume. This result is important in engineering operations such as molding or extrusion, when operations too close to T_g can result in a stiffening of the material. Investigation of the glass transitions of polymers under pressure is not a simple problem, especially in the case of elastomers whose T_g are usually well below the ambient temperature. In this case, the traditional pressure-transmitting fluid, Hg, must be replaced because its crystallization temperature is relatively high (i.e., 235.45 K). The choice of the replacement fluid is a challenge because it should be chemically inert with respect to the investigated sample. Also, values of its thermomechanical coefficients, compressibility, κ_T, and thermal expansivity, α_p, should be smaller than those of investigated samples. An additional difficulty in investigation of second-order-type transitions is the relatively weak effect measured. It is well known that the amplitude of the heat flux at the glass transition T_g increases with the temperature scanning rate while the time-constant of heat-flow-type calorimeters imposes temperature scan rates that are slow compared to typical DSC scan rates. However, with the use of an ultracryostat (see Fig. 1), we have used an appropriate temperature program for scanning temperature. This means that the temperature of the cooling liquid is lower than that of the calorimetric block during the stabilization periods (isothermal segments) and higher during the dynamic segment. In such a way, the scanning rate could be increased to 0.7 K min^{-1}, always keeping a minimal difference between target and real temperatures of the calorimetric block. Since the temperature gradient between the "heating fluid" and the calorimetric block was kept constant (20 K), the power uptake of the heating elements was quasi-constant, so the interference of sudden changes of power uptake on the calorimetric signal was avoided. The calorimetric response of a poly(butadiene-*co*-styrene) vulcanized rubber during isobaric scanning of temperature at 50 MPa with temperature ranging from 218.15 to 278.15 K at 0.4 K min^{-1} is illustrated in Fig. 3.

Figure 3 shows the evolution of T_g at different pressures, at 0.25, 10, 30, 50, and 90 MPa, respectively. As is seen in the insert of this figure, the T_g increases linearly with pressure with a slope of 0.193 ± 0.002 K MPa^{-1}. It should be noted that T_g is expressed as the temperature corresponding to the peak of the first derivative of the heat flux (i.e., the inflexion point of the heat flux).

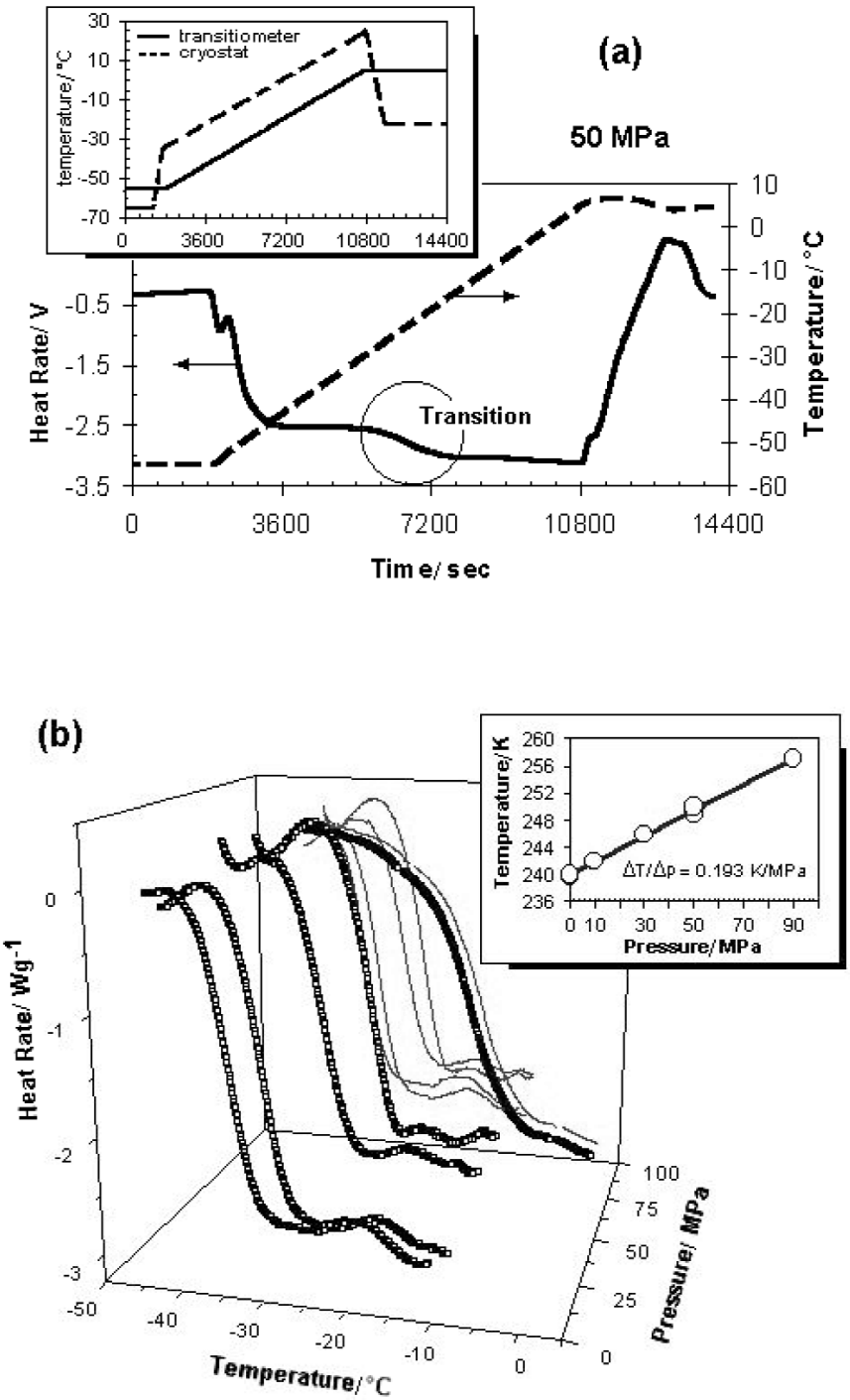

Fig. 3 Low-temperature, high-pressure investigation of a polymer glass transition by scanning transitiometry: (a) experimental thermogram obtained during an isobaric temperature scan at 50 MPa (styrene-butadiene rubber, SBR, sample mass = 1.56 g, scanning rate 0.4 K min^{-1}). In the inset, the temperature program for the transitiometer (full line) and heat transfer fluid (dashed line) are shown; (b) evolution with pressure of the glass-transition temperature (T_g –inflexion curve). The pressure coefficient, 0.193 K MPa^{-1}, of the glass-transition temperature is given in the inset.

Polymer particle synthesis using spectrotransitiometry

In the case of polymer synthesis, the scanning transitiometer is used as a reaction calorimeter, in which the advancement of a polymerization reaction is accurately monitored through rigorous control of the thermodynamic parameters. The differential configuration allows elimination of most of the systematic errors related to the experiment and/or heat transfer. The small thermal resistance makes it possible to work in a quasi-isothermal regime without power compensation, which is another major advantage of the present configuration. Results obtained from such measurements are to a large extent independent of the wetted surface or the stability of heat transfer, so that viscosity, minor changes in stirrer speed, and evaporation do not have to be taken into account here. To gather additional information on a reaction, we developed a reaction cell which combines in situ UV/Vis/NIR spectrometry, making use of a small optical probe coupled to a miniaturized spectrometer. In addition, the cell accommodates a stirrer and injection capillaries, allowing different dosing profiles for one or two reactants (see Fig. 2).

The performance of such instrumented transitiometer (i.e., *spectrotransitiometer*) is illustrated in the case of a process to which traditional reaction calorimetry was difficult to apply, such as precipitant polymerization, particularly the ultrafine polyamide (PA) particles synthesis by anionic polymerization of lactams in aprotic solvents. Anionic polymerization of lactams in organic solvents is a complex process. The most important steps in granular or powder PA formation are: initiation and growth of macromolecules in homogeneous medium, nucleation, phase separation and aggregation of the growing chains, solidification, and, finally, polymer crystallization. All of these events occur rapidly and partially overlap [26]. The polymerization occurs by the activated monomer mechanism, which supposes a two-step propagation mechanism involving the acylation of the lactam anion (NaL) by the *N*-acyllactam end-group of the growing chain followed by a fast proton-exchange with the monomer. The net result of each propagation step is the incorporation of a monomer unit into the polymer chain and the regeneration of the two active species [27]. In order to avoid the slow initiation step, the preformed *N*-acyllactams or their precursors (so-called chain initiators, CIs) are introduced in the system. In the very strong basic medium, the CI goes rapidly in side-reactions (Claisen condensation) and the polymerization is prematurely stopped [28]. Consequently, as long as monomer remains in the reaction medium, the polymerization can be continued simply by adding more CI. In other words, the polymerization can be stopped and restarted by controlling the amount of CI. A detailed analysis of the strong temperature influence has been possible through measuring heat flux under isothermal conditions, at four successive temperatures or nonisothermal conditions (i.e., by temperature scanning). Noticeably, the shape of the curves representing the heat evolution with polymerization passes from two peaks at low temperatures (up to 363 K) to a large shoulder that diminishes around 375 K, and finally disappears at high temperature (above 393 K) [14]. The area of the first peak is not influenced by temperature, but the area of the second one strongly increases with temperature, and, consequently, the monomer conversion increases too.

Using in situ Vis spectrometry (see Fig. 4) it was established that the first peak corresponds to the initiation reaction, i.e., between the two catalytic species (a very fast reaction), while the second one is the thermal contribution of the propagation reaction and of polymer crystallization during the phase separation. Under nonisothermal conditions (temperature scanning) the same trend of heat evolution was observed. A 3D representation of the spectrometric signal evolution versus time at 363 K is given in Fig. 4a. It is worth noting the stability of light transmission in the homogenous medium and its sharp decrease at the beginning of phase separation (polymer precipitation). The combination of the two signals, Fig. 4b, clearly demonstrates that the second peak arises almost at the same time as the phase separation.

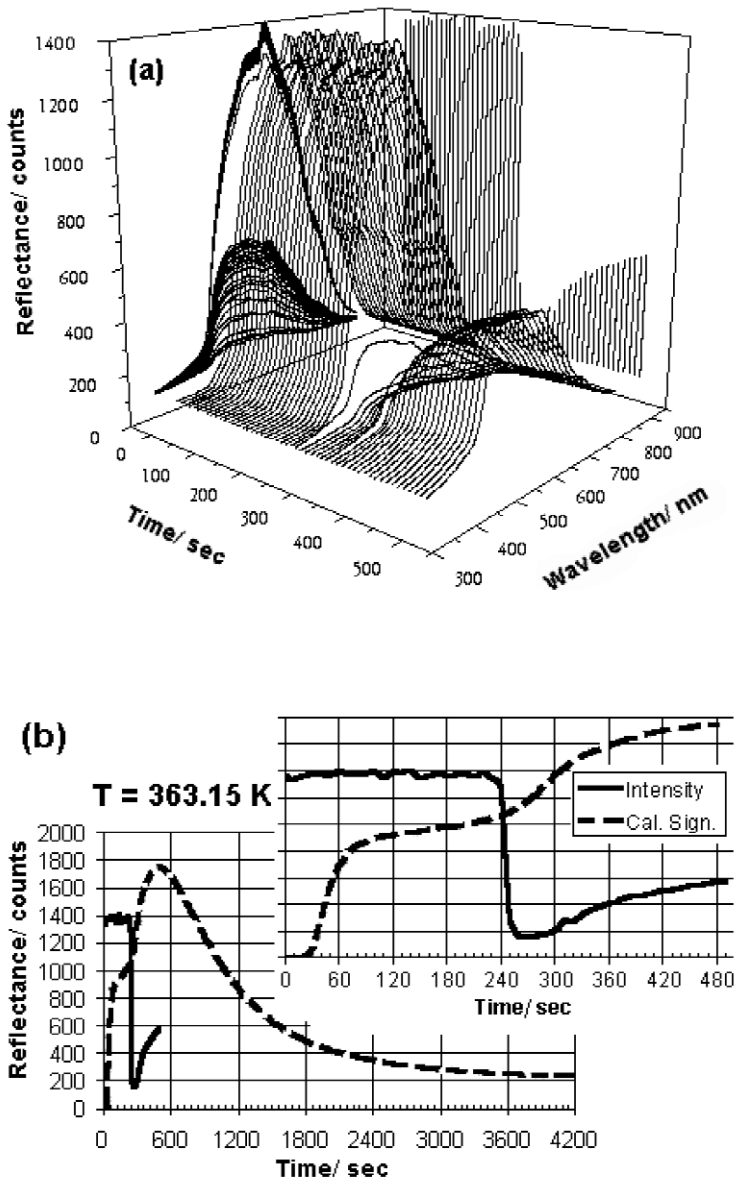

Fig. 4 Simultaneous in situ calorimetric and spectroscopic signals obtained with spectrotransitiometry: (a) 3D plots of the evolution of the spectrometric signal during anionic polymerization of caprolactam; (b) calorimetric and spectrometric signals recorded during polymerization at 363 K (the spectrometric signal was taken at 600 nm). Note the stability of the spectrometric signal before the phase separation and its sharp decrease at phase separation.

The main advantage of this process, as clearly demonstrated by spectrotransitiometry, is related to the possibility of orienting it toward the preparation of powders with desired morphologies through a fine-tuning of the synthesis parameters. To this goal, it was shown that one of the most convenient modalities is to continuously deliver the CI over a long period (Fig. 5a) [7]. In the case of continuous addition of CI, three important indications are provided by the spectrometric data, Fig. 5b. The first one (I in Fig. 5b) concerns the period between the start of reaction and the beginning of polymer precipitation; it depends on temperature and on the injection rate of CI. The second one (II in Fig. 5b) is related

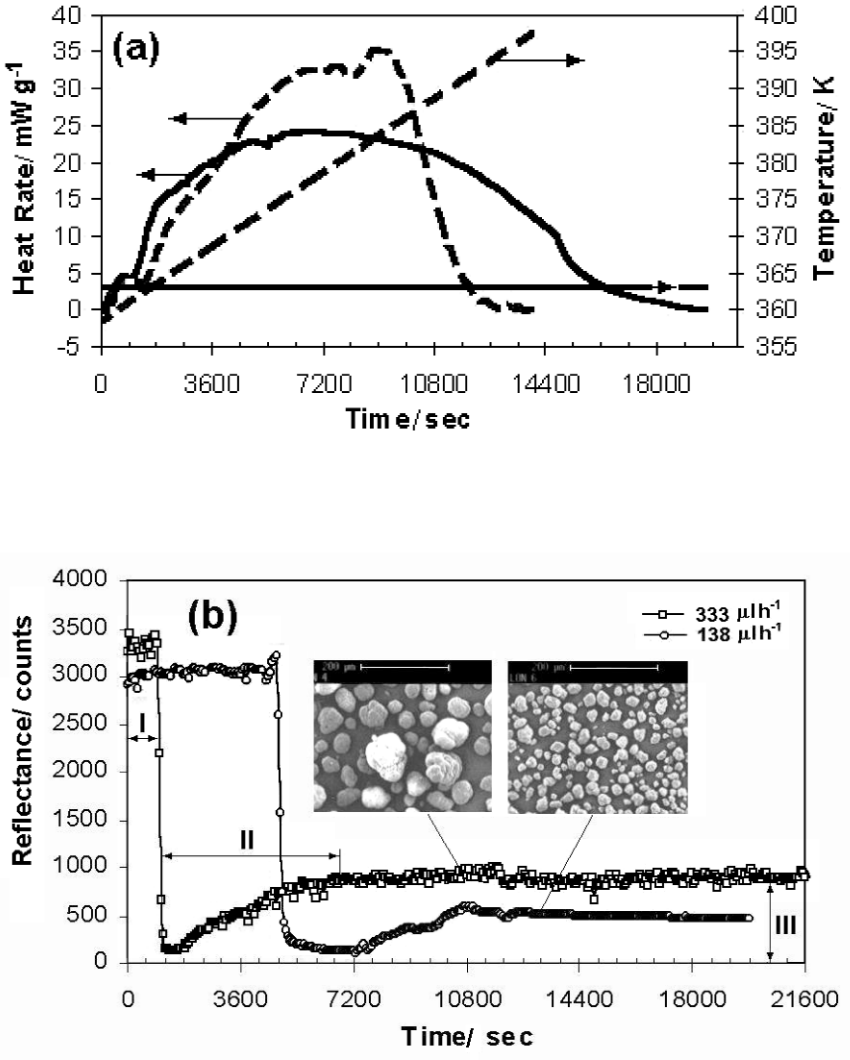

Fig. 5 The use of reaction calorimetry as a tool for process optimization: (a) controlled evolution of the heat rate by continuous addition of CI over a preestablished period, here 4 h with a rate of 60 µl h^{-1} under isothermal (solid lines) and nonisothermal conditions (dashed lines); (b) online qualitative development of particles and of their final size based on evolution of the spectrometric signal for different rates of feeding of CI, i.e., 138 and 333 µl h^{-1}, respectively. The reaction temperature was 378 K, and the intensity of the spectrometric signal was recorded at 600 nm. In the insets, the corresponding SEM micrographs of the obtained particles are given.

to the particle size evolution with time (this is only qualitative information). Generally, after phase separation, the evolution of spectrometric signal runs parallel to the conversion. As is seen in Fig. 5b, when one approaches the end of the process, the intensity of the spectrometric signal remains constant. Finally, the third piece of information (also qualitative) refers to the average size of particles. It was proved by SEM (see inserts of Fig. 5b) that the average particle size is directly proportional to the final intensity of spectrometric signal (III in Fig. 5b).

T_g determination by TMDSC of PS modified by high-pressure methane

There is not much information available in the literature on calorimetric study of plasticization of polymers at high pressures, above, say, 50 MPa, induced by gases. Plasticization is well characterized by the shift of the temperature of the glass transition, T_g. Actually, when pressure is induced by a gas, both plasticization and hydrostatic effects contribute to the shift of T_g. If plasticization tends to lower T_g because of the gain of mobility of the polymeric chains, the hydrostatic effect raises it in diminishing the free volume. Methane (CH_4) is assumed to be a nonplasticizing gas, but our results show that at higher pressures, plasticization overtakes again the hydrostatic effect, owing to a probably higher solubility of the gas in PS at higher pressures; this kind of behavior has been suggested for high enough pressures [24]. The plasticization of PS using CH_4 seems to be possible, but it is necessary to apply high pressure (i.e., 200 MPa) in order to obtain approximately the same shift of the T_g as with ethylene (C_2H_4) under 9.0 MPa! In this respect, CH_4 cannot really be considered as a good plasticizing gas. However, determination of the density of a PS sample "modified" under 200 MPa of methane has the characteristics of a foam, with a decrease of density of about 25 %. A comparison of PS samples modified by high pressure transmitted either by Hg or by methane (CH_4) has been studied at atmospheric pressure by TMDSC under the same conditions of modulation, that is to say, with amplitude A_T = 0.5 K, period p = 60 s, and average scanning rate q = 2 K min^{-1}, using a Mettler DSC 821. The results illustrate the capability of the technique to separate the glass transition from the relaxation phenomena that overlap. This separation, shown in Fig. 6 for a PS sample pressurized to 150 MPa by ("inert") Hg, enables us to not only determine the exact temperature of the glass transition of the sample through the reversing heat flow, but also to quantitatively evaluate the polymer history, in terms of thermal, mechanical, or chemical contributions. This information is "contained" in the peak (the minimum) exhibited by the non-reversing heat flow; integration of this peak yields the amount of energy quantifying then the non-reversing changes undergone by the sample.

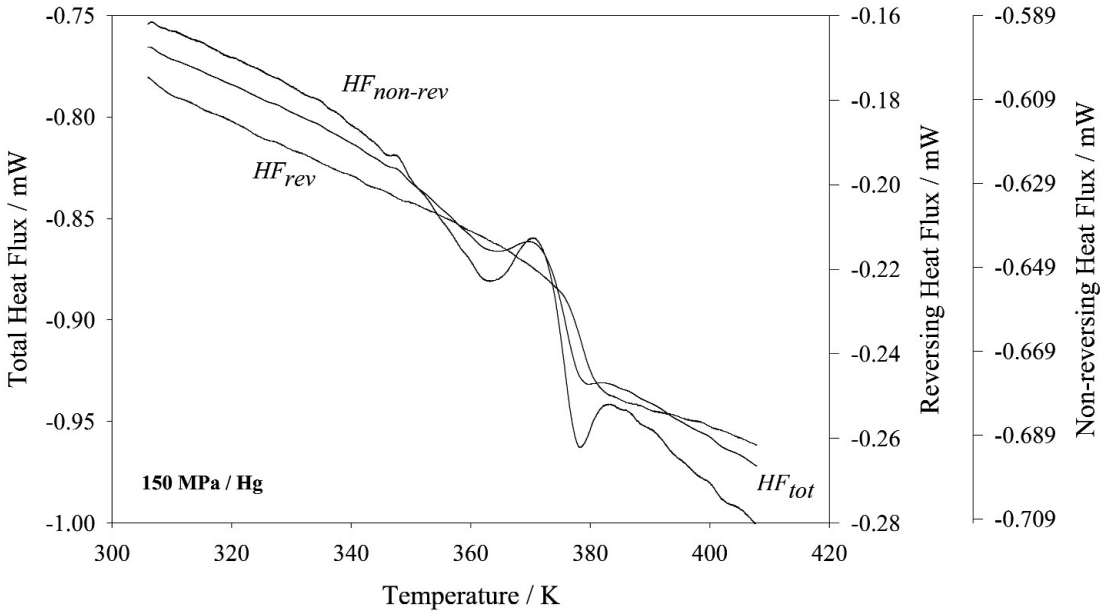

Fig. 6 TMDSC thermograms of PS modified by high pressure transmitted directly to the sample through Hg. The reversing heat flux HF_{rev} shows clearly the glass-transition inflexion curve.

It has been also shown that accurate results can be obtained with a specific mode of modulation, called quasi-isothermal mode [24]. Using this particular profile of the scanning rate, the equilibrium state can be approached and maintained since only a small thermal perturbation is applied to the sample. As a matter of fact, a small modulation is superimposed to an isotherm, in such a way that the mean scanning rate is zero. For the study of the glass transition, these conditions seem to be well suited since the same temperature of the transition can be obtained on heating as on cooling, which is never the case in classical DSC runs because of the crossing from metastable state (frozen) to equilibrium state (liquid). In this way, the benefits of the technique can be gained using advantageously the continuous mode of modulation, and we can determine not only the glass-transition temperatures of different samples of PS but also the corresponding enthalpies of relaxation. Samples of PS submitted to different pressures induced by Hg maintain their glassy aspect. TMDSC measurements yielded an identical glass-transition temperature independently of the pressure applied (50 or 150 MPa); this shows that, if the temperature of the glass transition varies during temperature scans under pressure, it is not modified in an irreversible manner by pressure. These results are not surprising; the hydrostatic pressure to which the sample is submitted does not modify the internal structure of the PS since there is no real interaction between Hg and PS. The increase of the glass-transition temperature, during measurements under pressure of Hg, is only due to the decrease of the free volume. This effect being reversible, the free volume increases again when the PS is decompressed until atmospheric pressure and the energy barrier between the two states, glassy and liquid, is crossed again at the same temperature. Although the interactions between methane and PS are weak, measurements realized under CH_4 have led to modifications of the sample. Figure 7 shows the curves obtained by TMDSC for PS modified under methane at 150 MPa. Remarkably, the temperature of the glass transition does remain identical, independent of the pressure of methane. This transition undergone by the sample seems to be reversible, not only for PS treated under hydrostatic pressures induced by Hg, but also for PS modified by high-pressure methane. Most likely, methane behaves as a solvent of PS; it tends to "lubricate" the chains of the polymer, increasing their mobility and leading then to a decrease of the glass-transition temperature during runs performed under pressures. After decompression, the mobility of the chains is limited again and T_g stays un-

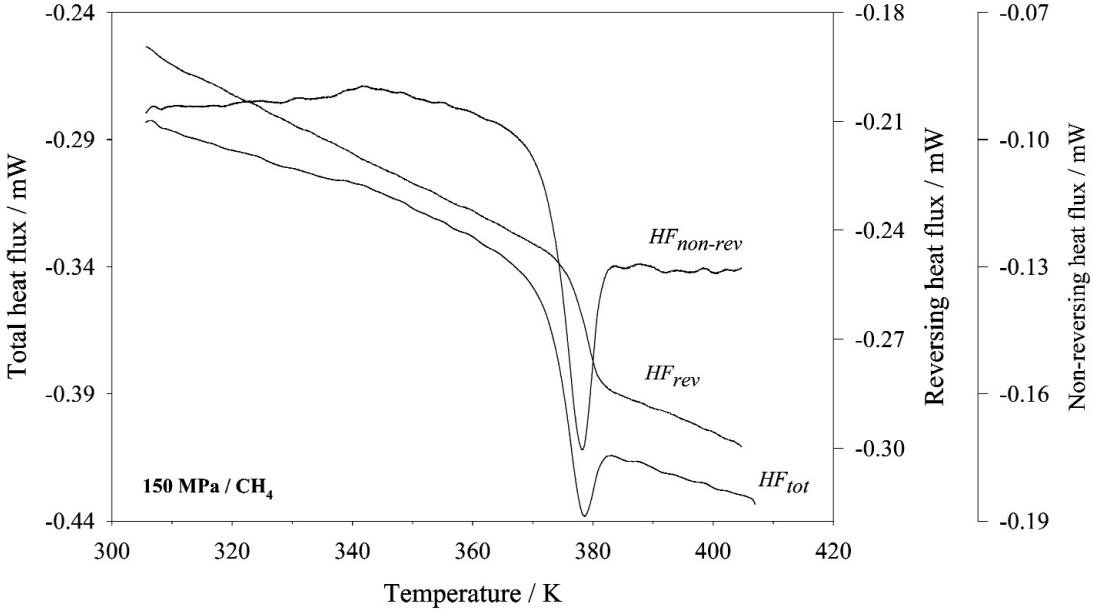

Fig. 7 TMDSC thermograms of PS modified by high pressure transmitted directly to the sample through CH_4. The reversing heat flux HF_{rev} shows clearly the glass-transition inflexion curve.

changed. The modifications of the aspect (opacity) are a direct result of the foaming effect. The only changes that can be noticed, by comparison with the initial PS, appear in the non-reversing signals. As a result of the constraints applied to the polymer, that is, thermal (the same for all samples), mechanical, and chemical, the effect of pressure can be observed as a main endothermic peak in the non-reversing heat flow. The quasi disappearance of the first peak (as seen on Fig. 6) can be explained by an increase of the enthalpy of the polymer due to the gas sorption. As a matter of fact, the thermograms obtained after an identical study on one-year-old (CH_4-treated) samples, that is, on samples after possible partial diffusion of the gas, show that a sub-T_g peak does still appear [24].

CO_2 solubilities in MDPE and PVDF

The sorption of carbon dioxide in MDPE was measured along three isotherms up to a pressure of 43 MPa for both sorption and desorption. Measurements were performed on solid polymers of two different types of samples (circular cross-section rods): a number of thin rods (length 65.0 mm, diameter 2.1 mm, and total mass 3.750 g) at 333.15 and 338.15 K, one single rod (length 74.7 mm, diameter 4.4 mm, and mass 1.048 g) at 353.15 K. Figure 8 shows measurements taken at 338.15 K.

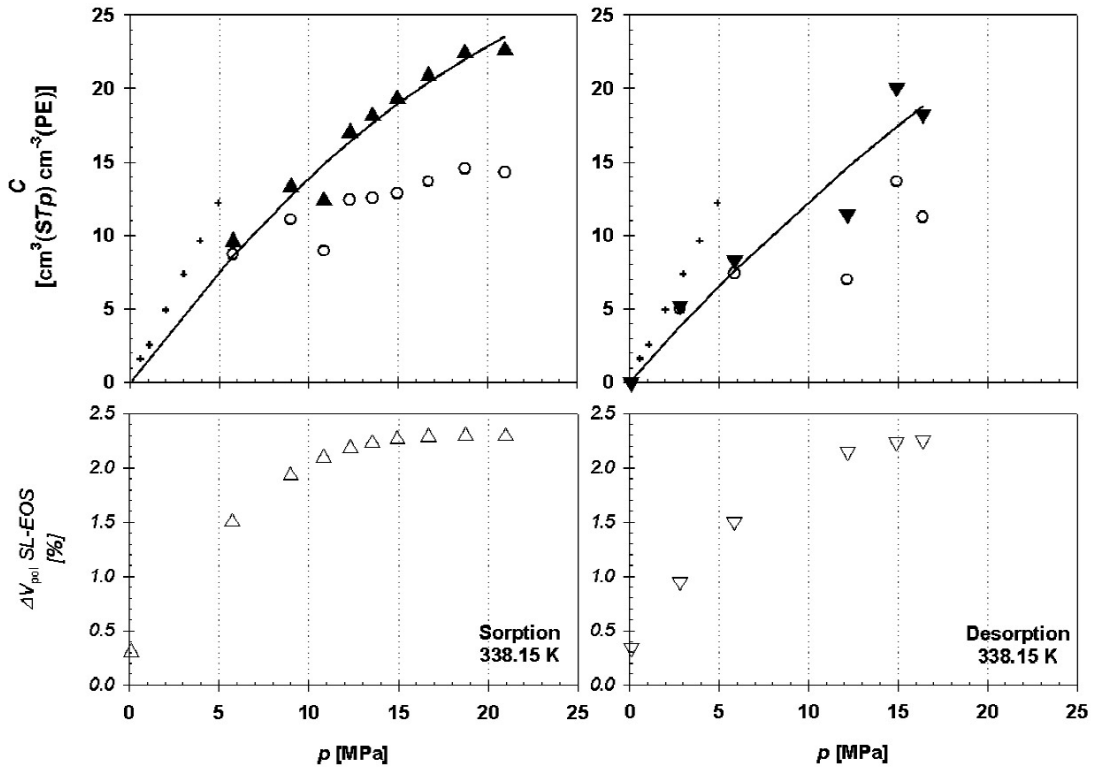

Fig. 8 Sorption (left-hand side) and desorption (right-hand side) of CO_2 up to 25 MPa in MDPE at 338.15 K. Presented as functions of pressure, the apparent concentrations (open circles) and corrected values (closed triangles) calculated using the swelling ΔV_{pol} of the polymer estimated with the SL-EOS (open triangles in lower graphs). Fit of the corrected values (solid lines) is made with the "dual-mode" model. **+**, Kamiya et al. [29] at 308.15 K for LDPE.

Estimation of the change in volume of the polymer was made [12] with the SL-EOS. The correction of the polymer swelling amounts from 4 to 2.5 % depending on the temperature. As expected, swelling increases with solubility and tends to a limit. This tendency would be explained by an increase of the free volume accessible to a penetrant molecule: that is, a CO_2-induced increase in total free volume or a redistribution of existing free volume. The correlation of the corrected concentration during sorption and desorption of CO_2 in MDPE was made [12] using the "dual-mode" model. The gas concentration increases with increasing pressure and seems to decrease with increasing temperature. The only literature data for sorption in PE block samples are from Kamiya et al. [29]. They investigated sorption and desorption of CO_2 in low-density polyethylene (LDPE) using a gravimetric method up to 5 MPa at 308.15 K. Our measurements taken in the same conditions are in good agreement with their results.

Two isotherms for the sorption of carbon dioxide in PVDF at 391.15 K are shown on Fig. 9. Measurements were performed on solid polymers of two different types of samples (rods): a number of circular cross-section rods (length 58.1 mm, diameter 2.4 mm, and total mass 5.716 g) and a single rectangular cross-section rod (length 69.9 mm, width 8.8 mm, thickness 5.1 mm, and mass 5.588 g). An apparent convex curve is obtained different from what was observed with MDPE. The apparent concentration goes through a maximum, 18 [cm^3 (STP) cm^{-3} (PVDF)], at 10 MPa, and then decreases with pressure. A similar trend was observed with two different studies. These series of data attest to the reliability of the apparatus. As regards experimental uncertainties, this indicates that the geometry of sam-

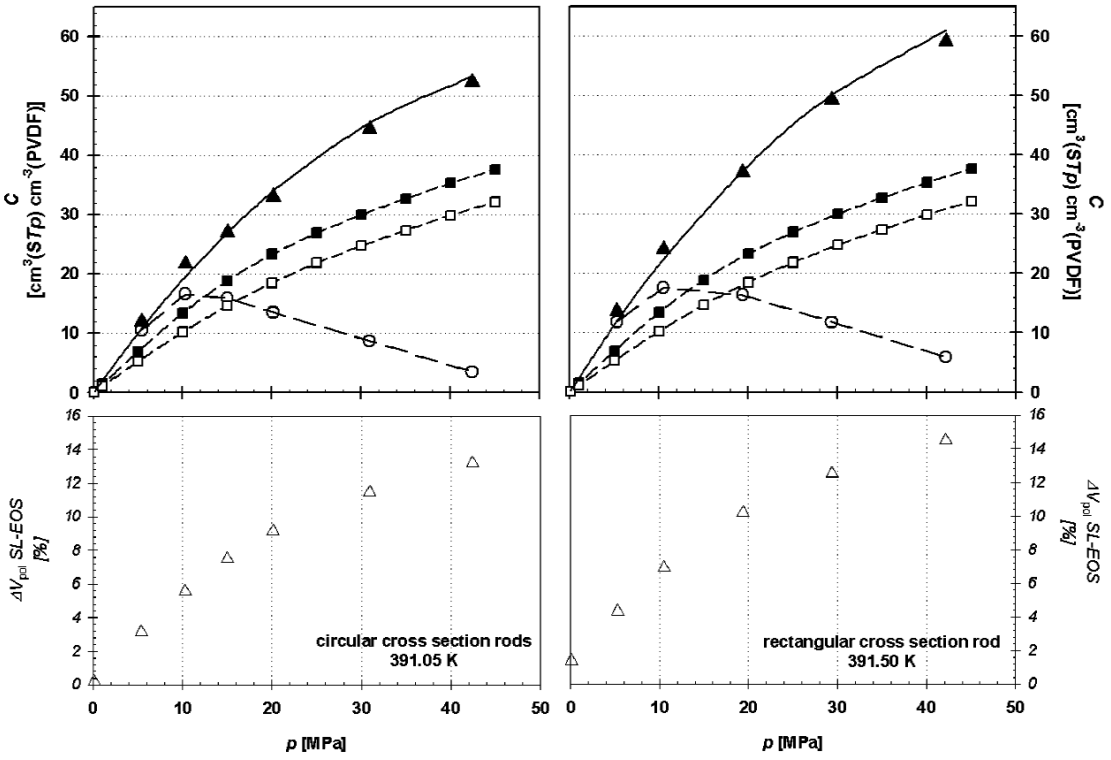

Fig. 9 Apparent concentrations (open circles) of CO_2 in PVDF at 391.15 K as a function of pressure (up to 43 MPa) in two different types of polymer samples (circular cross-section rods and rectangular cross-section rod). Plotted as functions of pressure, the apparent concentrations (open circles) and corrected values (closed triangles) calculated using the swelling ΔV_{pol} of the polymer estimated with the SL-EOS (open triangles in lower graphs). The correlation (solid lines) of the corrected values is done using the "dual-mode" model. Data of Rodgers [30]: at 373.15 K (closed squares) and at 398.15 K (open squares).

ple does not influence in a significant way the concentration of the gas as long as the system is at the thermodynamic equilibrium.

The apparent concentration of CO_2 in PVDF, higher than in MDPE, could be attributed to the uncertainty when calculating the polymer swelling with the SL-EOS. These calculations yield a variation in volume of 14 % at 42 MPa. The corrected concentration in the sorption mode is fitted with the "dual mode" [12]. Quantitative comparison with the work of Rodgers [30], who studied the same type of polymer under supercritical CO_2 at 373.15 and 398.15 K, confirms that the apparent concentration is underestimated as a consequence of the significant contribution of the swelling. At low pressures, up to 10 MPa, neglecting swelling does not affect the solubility, but above 15 MPa the change in volume seems important and cannot be ignored. The conclusion is in good agreement with that of Lorge et al. [31] as regards the variation of mass and the corresponding volume change for the CO_2-PVDF system at 353.15 K, during sorption and desorption at a speed of 0.5 MPa min^{-1}. They determined the gaseous mass uptake using a vibrating-beam technique, the dilatation studies being performed using an ultrasonic transducer. Recent calorimetric investigations by Grolier et al. [14] confirm such trend connecting gas solubility, swelling of the polymer during sorption, and the associated energy of interaction.

CONCLUSION

New developments in calorimetric techniques particularly in scanning transitiometry and associated techniques, like TMDSC or VW-*pVT* technique, have permitted notable broadening of the fields of applications in polymer thermodynamics, with incursions in several major domains. The first one deals with the determination of thermophysical properties of polymers pressurized either by an incompressible inert fluid (Hg) or by highly compressible gases (such as supercritical fluids). The second one concerns the effect of pressure in the presence or the absence of gases on different phase transitions (fusion/crystallization and glass transitions) over wide temperature and pressure ranges. The third one illustrates how scanning transitiometry and its new development, spectrotransitiometry, can be used as a versatile technique for online monitoring fine particle synthesis as well as particle size tuning. All these applications demonstrate what polymer thermodynamics has gained in recent years through the use of such techniques.

REFERENCES

1. S. L. Randzio. *Thermochim. Acta* **89**, 215 (1985).
2. S. L. Randzio, D. J. Eatough, E. A. Lewis, L. D. Hansen. *J. Chem. Thermodyn.* **20**, 937 (1988).
3. S. L. Randzio. *Pure Appl. Chem.* **63**, 1409 (1991).
4. S. L. Randzio, J.-P. E. Grolier, J. R. Quint. *Rev. Sci. Instrum*. **65**, 960 (1994).
5. S. L. Randzio, J.-P. E. Grolier, J. Zaslona, J. R. Quint. French Patent 91-09227, Polish Patent P-295285.
6. S. L. Randzio, Ch. Stachowiak, J.-P. E. Grolier. *J. Chem. Thermodyn.* **35**, 639 (2003).
7. F. Dan and J.-P.E. Grolier. *Setaram News* **7**, 13 (2002).
8. M. Reading, D. Elliott, V. L. Hill. *J. Therm. Anal*. **40**, 949 (1993).
9. J. E. K. Schawe. *Thermochim. Acta* **261**, 183 (1995).
10. S. Hilic, A. A. H. Padua, J.-P.E. Grolier. *Rev. Sci. Instrum*. **71**, 4236 (2000).
11. S. Hilic, S. A. E Boyer, A. A. H. Padua, J.-P.E. Grolier. *J. Polym. Sci. B: Polym. Phys.* **39**, 2063 (2001).
12. S. A. E. Boyer and J.-P.E. Grolier. *Polymer* **46**, 3737 (2005).
13. S. L. Randzio. *J. Therm. Anal. Cal*. **57**, 165 (1999).
14. J.-P.E. Grolier, F. Dan, S. A. E. Boyer, M. Orlowska, S. L. Randzio. *Int. J. Thermophys.* **25**, 297 (2004).
15. S. L. Randzio, I. Flis-Kabulska, J.-P.E. Grolier. *Macromolecules* **35**, 8852 (2002).

16. S. L. Randzio, I. Flis-Kabulska, J.-P.E. Grolier. *Biomacromolecules* **4**, 937 (2003).
17. M. Orlowska, S. L. Randzio, J.-P.E. Grolier. *In Advances in High Pressure Bioscience and Biotechnology*, R. Winter (Ed.), Springer, Berlin (2003).
18. S. L. Randzio and J.-P. E. Grolier. *Anal. Chem.* **70**, 2327 (1998).
19. F. Dan and J.-P.E. Grolier. In *Chemical Thermodynamics for Industry*, T. M. Letcher (Ed.), Royal Society of Chemistry, London (2004).
20. J.-P.E. Grolier and F. Dan. In *8th International Workshop on Polymer Reaction Engineering*, H.-U. Moritz and K.-H. Reichert (Eds.), Dechema Monographs, Vol. 138, John Wiley-VCH, Frankfurt (2004).
21. M. Ribeiro, J-P.E. Grolier, L. Pain, C. Gourgon. *USERCOM* **1**, 12 (2002).
22. L. Pain, C. Higgins, B. Scarfoglières, S. Tedesco, B. Dal'Zotto, C. Gourgon, M. Rebeiro, T. Kusumoto, M. Suetsugu, R. Hanawa. *J. Vac. Sci. Technol.* **B18** (8), 3388 (2000).
23. C. Perret, C. Gourgon, G. Micouin, J.-P. E. Grolier. *Jpn. J. Appl. Phys.* **41**, 4203 (2002).
24. M. Ribeiro, L. Pison, J.-P. E. Grolier. *Polymer* **42**, 1653 (2001).
25. S. A. E. Boyer and J.-P. E. Grolier. *Pure Appl. Chem.* **77**, 593 (2005).
26. F. Dan and C. Vasiliu-Oprea. *Colloid Polym. Sci.* **276**, 483 (1998).
27. H. Sekiguchi. In *Ring-Opening Polymerization* Vol. 2, K. J. Iving and T. Saegusa (Eds.), p. 833, Elsevier, London (1984).
28. J. Stehlicek and J. Sebenda. *Eur. Polym. J.* **22**, 769 (1986).
29. Y. Kamiya, T. Hirose, K. Mizoguchi, Y. Naito. *J. Polym. Sci. B: Polym. Phys.* **24**, 1525 (1986).
30. P. Rodgers. *IFP (Institut Français du Pétrole)* Report 39887 (July 1992).
31. O. Lorge, B. J. Briscoe, P. Dang. *Polymer* **40**, 2981 (1999).